Frame Error Probability of Frequency-Flat Block Fading Channels with Frame Repetition

Marc Sanchez Net*

ABSTRACT. — This article studies the frame error probability of frequency-flat block fading channels assuming that no interleavers are used at the transmitter and receiver. This assumption is typically applicable for very slow fading channels, where interleaving is not possible because it requires too much storage or it introduces too much delay. In the context of space exploration, such channels can occur between landed spacecraft on the lunar or Martian surface and a Deep Space Network station, as shown by our previous work.

Two figures of merit are considered: First, we study the frame error probability for a link impaired by frequency-flat multi-path fading effects where data is transmitted using traditional forward error correction codes. Then, we extend the analysis to estimate this same quantity if a second copy of each coded frame is sent after a fixed time delay, i.e., errors due to fade events are protected through a combination of coding and repetition. We demonstrate that using this hybrid approach can significantly improve link performance (measured in terms of E_b/N_0 for a given frame error rate) and is therefore a good alternative for links where interleaving is impractical.

I. Introduction

In a previous article we studied the multi-path fading effects affecting a link between a rover on the lunar South Pole and a Deep Space Network (DSN) antenna [1]. We showed that, assuming moderate data rates (between 1 kbps and 0.5 Mbps), the link can be modeled as a frequency-flat fading channel that with a Gaussian-shaped power spectral density (PSD). We also showed that the channel coherence time is large (on

*Communications Architectures and Research Section.

The research described in this publication was carried out by the Jet Propulsion Laboratory, California Institute of Technology, under a contract with the National Aeronautics and Space Administration.

the order of 50 msec) compared to the symbol duration time, which led to the conclusion that the fading process is slow-varying.

In this article, we study the frame error probability of this type of channel under the assumption of block fading and no interleaving. In other words, we consider that deep fades in the system last long enough to wipe out entire frames and, consequently, the channel can be approximated as an ON/OFF process. Note that this approximation is only valid if the duration of a frame is significantly smaller than the channel's coherence time. For instance, a lunar rover transmitting 1024 low density parity-check (LDPC) frames at 500 kbps using a binary phase-shift keying (BPSK) modulation will transmit an entire frame with 2.05 msec approximately. Therefore, if the coherence time is 50 msec, then the system will effectively experience block fading.

The results of this article can be applied in at least two practical settings: On the one hand, the transmitter can transmit copies of any given frame after a given delay and tag each of them with a sequence number, which is then used by the receiver to identify and discard any secondary copies it correctly decodes. On the other hand, this multi-copy scheme can be used in combination with an Automatic Repeat reQuest mechanism (e.g., the Licklider Transmission Protocol) to increase errorless system throughput. Indeed, it is well-known that feedback can increase capacity if the channel has memory (as is the case with fading channels), and the feedback is not provided to the transmitter instantaneously [2].

The reminder of this paper is organized as follows: First, we formalize the received signal, channel and receiver models, including the fading channel approximation as an ON/OFF process. We then show how this simplified system model can be used to estimate Frame Error Rate (FER) curves as a function of signal-to-noise rate (SNR), and provide their asymptotic behavior. Then, we extend the analysis to consider a communication scheme in which multiple copies of a frame are sent over the channel delayed in time by τ seconds. Finally, we conclude by applying our results to a link between the lunar South Pole and a DSN station.

II. System Model

A. Signal Model

We consider that the transmitter sends a BPSK signal with residual carrier. Therefore, the complex baseband equivalent of received signal at the DSN station can be expressed as [3]

$$r(t) = \sqrt{P_r} F(t) e^{j[2\pi(f_c + f_d + r_d(t))t + \beta m(t) g(t) + \theta_c]} + n(t), \tag{1}$$

where P_r is the total received signal power, $m(t) = \sum_{k=-\infty}^{\infty} a_k p(t - kT_s)$ represents the BPSK modulated signal with the k-th bit taking on values $a_k \in \{+1, -1\}$, $p(t)$ is a unit-power rectangular pulse of duration T_s, f_c and θ_c denote the carrier frequency and phase respectively, f_d represents the Doppler frequency shift, and $r_d(t)$ is the

Doppler rate. Data is modulated onto a subcarrier of either square or sine waveform, i.e., $g(t) = \text{sign}\,(2\pi f_{sc} t)$ or $g(t) = \sin\,(2\pi f_{sc} t)$, using a modulation index $\beta < 90\,\text{deg}$. Finally, $n(t)$ is a zero mean complex Additive White Gaussian Noise (AWGN) with two-sided power spectral density $\frac{N_0}{2}$, and $F(t)$ denotes the complex fading process.

B. Fading Process Model

Based on our previous article, we consider that the channel can be modeled as a normalized complex Gaussian process $F(t)$ such that

$$F(t) = F_I(t) + jF_Q(t), \tag{2}$$

where

$$F_I(t) \sim \mathcal{N}(s\cos\left[2\pi\left(f_c + f_d + r_d(t)\right)t\right], b_0) \tag{3}$$
$$F_Q(t) \sim \mathcal{N}(s\sin\left[2\pi\left(f_c + f_d + r_d(t)\right)t\right], b_0), \tag{4}$$

b_0 and s measure the strength of the scattered and LoS rays respectively (in units of power), and $\Omega_p = s^2 + 2b_0$ is normalized to 1. Additionally, the second-order moments of the stochastic process are given by a Gaussian power spectral density function such that

$$S(f) \approx \frac{b_0}{\sqrt{2\pi}\sigma_f} e^{-\frac{(f-f_d)^2}{2\sigma_f^2}}, \tag{5}$$

where σ_f is the Doppler spread or, equivalently, the inverse of the channel's coherence time [4].

It is sometimes useful to parameterize this fading channel using a complimentary set of variables. In particular, if we define the *Rice factor* as $K = s^2/2b_0$, then the channel is said to experience Rayleigh fading if $K = 0$, while Rician fading occurs for $K > 0$. Additionally, the probability density functions for the fading envelope and power, denoted $\alpha(t) = |F(t)|$ and $\alpha^2(t)$ respectively, are known to be

$$p_\alpha\left(x\right) = \frac{x}{b_0} e^{-\frac{x^2}{2b_0}} \tag{6}$$
$$p_{\alpha^2}\left(x\right) = \frac{1}{2b_0} e^{-\frac{x}{2b_0}}, \tag{7}$$

for Rayleigh fading, and

$$p_\alpha\left(x\right) = \frac{x}{b_0} e^{-\frac{x^2+s^2}{2b_0}} I_0\left(\frac{xs}{b_0}\right) \tag{8}$$
$$p_{\alpha^2}\left(x\right) = \frac{1}{2b_0} e^{-\frac{x+s^2}{2b_0}} I_0\left(\frac{s\sqrt{x}}{b_0}\right), \tag{9}$$

for Rician fading.

C. Receiver Model

We model the DSN antenna receiving subsystem as an idealized system where the Phased-Lock Loop provides perfect carrier synchronization and timing. We also assume that the fading process $F(t)$ is slow varying such that, at any point in time, the instantaneous channel SNR is experienced by all symbols within a codeword. Therefore, the average frame error rate at the receiver output will depend on the fading-corrected SNR $\zeta(t) = \alpha^2(t)\gamma$, where γ denotes the energy per bit to spectral noise density ratio of the constant AWGN noise.

Let $f(\gamma)$ denote the characteristic curve of the code used in the system assuming the channel is only affected by AWGN noise. Then, in the presence of slow block fading and without interleaving, the average FER can simply be estimated by using the fading-corrected signal-to-noise ratio instead:

$$\mathrm{FER}(\gamma) = \int_0^\infty f\left(\alpha^2\gamma\right) p_{\alpha^2}\left(\alpha^2\right) d\left(\alpha^2\right), \tag{10}$$

where $p_{\alpha^2}\left(\alpha^2\right)$ is the probability density function of the Rayleigh or Rician-distributed fading power. Unfortunately, no analytic expressions are generally available for $f(\cdot)$ and, therefore, we must resort to numerical integration to obtain any results. However, if $f(\cdot)$ has a sufficiently steep waterfall region and low-enough error floor, we can approximate its shape by an inverted heavy-side function such that

$$f\left(\alpha^2\gamma\right) \approx \begin{cases} 1 & \text{if } \alpha^2\gamma \leq \delta\Omega_p \\ 0 & \text{if } \alpha^2\gamma > \delta\Omega_p, \end{cases} \tag{11}$$

where δ is a constant that must be calibrated so that the FER error is minimized. Consequently, the average FER as a function of signal-to-noise ratio after this simplification becomes

$$\begin{aligned} \mathrm{FER}(\gamma) =& 1 \cdot P_{\alpha^2}\left(\alpha^2 \leq \tfrac{\delta\Omega_p}{\gamma}\right) + 0 \cdot P_{\alpha^2}\left(\alpha^2 > \tfrac{\delta\Omega_p}{\gamma}\right) \\ =& P_{\alpha^2}\left(\alpha^2 \leq \tfrac{\delta\Omega_p}{\gamma}\right) = P_\alpha\left(\alpha \leq \sqrt{\tfrac{\delta\Omega_p}{\gamma}}\right). \end{aligned} \tag{12}$$

In other words, we have modeled the system's performance as an ON/OFF channel where frame errors occur if and only if the fading envelope falls below a certain threshold (and vice versa). This threshold depends on the link's γ, as well as an empirical constant δ that must be calibrated for the code and receiver under consideration.

D. Definition of Energy per Bit in Multi-Copy Systems

Up until this point we have discussed the receiver performance in terms of the energy per *transmitted bit* to spectral noise density ratio γ. In traditional coded systems, where each frame is sent once, this value is simply estimated as the energy per symbol

to spectral noise density ratio minus the code rate, i.e., $\gamma_1 = \frac{E_s}{N_0} - R$ in logarithmic scale, where $R < 1$ denotes the code rate. Additionally, this quantity is also equal to the energy per *information bit* to spectral noise density ratio $\frac{E_b}{N_0}$, since each bit is only sent once.

The same idea applies to multi-copy systems. However, in this case each information bit is sent multiple times over the channel and, consequently, a *transmitted bit* is no longer equivalent to an *information bit*. Instead, the following relationship holds: $\frac{E_b}{N_0} = \gamma + n$, in logarithmic scale, where n denotes the number of times an information bit is sent over the channel. Notionally, the factor n accounts for the fact that the transmitter needs to spend n times more energy to transfer the same amount of information. Or, equivalently, the transmitter needs to send data at a rate n times faster than if no additional copies were sent.

For the purposes of this article, all equations presented in the following section are expressed in terms of γ rather than $\frac{E_b}{N_0}$ since they are slightly easier to work with. However, when we report the performance of multi-copy schemes and compare it to single-copy systems we translate all plots to $\frac{E_b}{N_0}$ to ensure that we utilize the same units.

III. Frame Error Probability

Let p_1 denote the frame error probability in a channel experiencing block fading and modeled as described in Section II.

Lemma 1. *Assume that the fading channel is Rayleigh distributed and a frame error occurs if and only if* $\alpha(t) \leq \sqrt{\frac{\delta\Omega_p}{\gamma}}$. *Then,*

$$p_1 = 1 - e^{-\frac{\delta}{\gamma}}. \tag{13}$$

The proof is given in Appendix A-A.

Lemma 2. *Assume that the fading channel is Rician distributed and a frame error occurs if and only if* $\alpha(t) \leq \sqrt{\frac{\delta\Omega_p}{\gamma}}$. *Then,*

$$p_1 = 1 - Q\left(\sqrt{2K}, \sqrt{2(K+1)\frac{\delta}{\gamma}}\right) \tag{14}$$

where $Q(a, b)$ *denotes the Marcum Q function. The proof is given in Appendix A-B.*

Lemma 3. *Consider a Rayleigh or Rician fading channel with arbitrary PSD. Then, as* $\gamma \to \infty$,

$$p_1 \sim \frac{1}{\gamma}. \tag{15}$$

The proof is a special case of Appendix C.

IV. Dual-Copy Frame Error Probability

Let p_1 denote the frame error probability in a channel experiencing block fading and modeled as described in Section II. Also, let p_2 be defined as the probability of dropping two copies of a frame that are sent τ seconds apart.

Lemma 4. *Assume that the fading channel is Rayleigh distributed and an error occurs if and only if $\alpha^2(t) \leq \frac{\delta\Omega_p}{\gamma}$. Let $\alpha_1 = \alpha(t)$ and $\alpha_2 = \alpha(t+\tau)$. Then,*

$$\begin{aligned} p_2 =& P\left(\alpha_1 \leq \sqrt{\tfrac{\delta\Omega_p}{\gamma}}, \alpha_2 \leq \sqrt{\tfrac{\delta\Omega_p}{\gamma}}\right) \\ =& \int_0^{\sqrt{\delta\Omega_p/\gamma}} \int_0^{\sqrt{\delta\Omega_p/\gamma}} \frac{\alpha_1\alpha_2}{A} e^{-\frac{b_0}{2A}\left(\alpha_1^2+\alpha_2^2\right)} I_0\left(\frac{\alpha_1\alpha_2}{A}\sqrt{\mu_1^2+\mu_2^2}\right) d\alpha_1 d\alpha_2, \end{aligned} \tag{16}$$

where

$$A = b_0^2 - \mu_1^2 - \mu_2^2 \tag{17}$$

$$\mu_1(\tau) = \int_{-\infty}^{\infty} \cos\left(2\pi f\tau\right) df \tag{18}$$

$$\mu_2(\tau) = \int_{-\infty}^{\infty} \sin\left(2\pi f\tau\right) df. \tag{19}$$

The proof is given in Reference [5], Equation (3.7-13).

Lemma 5. *Assume the same conditions as in Lemma 4. Assume also that the fading channel is characterized by a Gaussian PSD as in Equation 5. Let $\tau_n = \frac{\tau}{T_c}$ denote the normalized delay and $\rho = e^{-2(\pi\tau_n)^2}$ denote the normalized correlation between two time instants separated by τ_n. Then,*

$$p_2 = p_1 - e^{-\frac{\delta}{\gamma}}\left[Q\left(z, z\rho\right) - Q\left(z\rho, z\right)\right] \tag{20}$$

with $z = \sqrt{\frac{2}{1-\rho^2}\frac{\delta}{\gamma}}$. The proof is given in Appendix B-A.

Corollary 5.1. *Assume the same conditions as in Lemma 5. Assume also that $\tau_n \geq \frac{1}{2}$. Then,*

$$p_2 \approx \left[1 - e^{-\frac{\delta}{\gamma}}\right]^2. \tag{21}$$

The proof is given at the end of Appendix B-A.

Lemma 6. *Assume that the fading channel is Rician distributed and an error occurs if and only if $\alpha^2(t) \leq \frac{\delta\Omega_p}{\gamma}$. Let $\alpha_1 = \alpha(t)$ and $\alpha_2 = \alpha(t+\tau)$. Then,*

$$p_2 = P\left(\alpha_1 \leq \sqrt{\tfrac{\delta\Omega_p}{\gamma}}, \alpha_2 \leq \sqrt{\tfrac{\delta\Omega_p}{\gamma}}\right) = \int_0^{\sqrt{\delta\Omega_p/\gamma}} \int_0^{\sqrt{\delta\Omega_p/\gamma}} f_{\boldsymbol{\alpha}}\left(\alpha_1, \alpha_2\right) d\alpha_1 d\alpha_2, \tag{22}$$

where

$$f_{\boldsymbol{\alpha}}(\alpha_1,\alpha_2)=\frac{\alpha_1\alpha_2}{(2\pi)^2 A}\int_0^{2\pi}\int_0^{2\pi} e^{-\frac{1}{A}\left[\frac{b_0}{2}z_1+s(\alpha_1 z_2+\alpha_2 z_3)-\alpha_1\alpha_2 z_4-s^2 z_5\right]}d\theta_1 d\theta_2 \tag{23}$$

and

$$z_1=\alpha_1^2+\alpha_2^2 \tag{24}$$

$$z_2=\mu_1\cos(\theta_1-\phi_\tau)+\mu_2\sin(\theta_1-\phi_\tau)-b_0\cos\theta_1 \tag{25}$$

$$z_3=\mu_1\cos\theta_2+\mu_2\sin\theta_2-b_0\cos(\theta_2-\phi_\tau) \tag{26}$$

$$z_4=\mu_1\cos(\theta_1-\theta_2)+\mu_2\sin(\theta_1-\theta_2) \tag{27}$$

$$z_5=\mu_1\cos\phi_\tau+\mu_2\sin\phi_\tau-b_0 \tag{28}$$

$$\phi_\tau=2\pi f_c\tau. \tag{29}$$

A, μ_1 and μ_2 are defined in Equations 17, 18 and 19 respectively. The proof is given in Appendix B-B.

Lemma 7. *Assume the same conditions as in Lemma 6. Assume also that the fading channel is characterized by a Gaussian PSD and define ρ as in Lemma 5. Then,*

$$p_2=p_1-\int_0^{\sqrt{\delta\Omega_p/\gamma}}\int_0^{2\pi}\frac{\alpha}{2\pi b_0}e^{-\frac{1}{2b_0}\left[\alpha^2-2\alpha s\cos\theta+s^2\right]}Q\left(\sqrt{\tfrac{2K}{1-\rho^2}}z_1,\sqrt{\tfrac{2(K+1)}{(1-\rho^2)}\tfrac{\delta}{\gamma}}\right)d\theta d\alpha \tag{30}$$

where

$$z_1(\alpha,\theta)=\sqrt{\left(\frac{\rho\alpha}{s}\right)^2+\frac{2\rho\alpha}{s}\left[\cos(\theta-\phi_\tau)-\rho\cos\theta\right]+1+\rho^2-2\rho\cos\phi_\tau}. \tag{31}$$

The proof is given in Appendix B-C.

Corollary 7.1. *Assume the same conditions as in Lemma 7. Assume also that $\tau_n\geq\frac{1}{2}$. Then,*

$$p_2\approx\left[1-Q\left(\sqrt{2K},\sqrt{2(K+1)\tfrac{\delta}{\gamma}}\right)\right]^2. \tag{32}$$

The proof is given in Appendix B-D.

Lemma 8. *Consider a Rayleigh or Rician fading channel with arbitrary PSD. Assume that a frame error occurs if and only if $\alpha^2(t)\leq\frac{\Omega_p}{\gamma}$ and both copies of a frame are lost. Then, as $\gamma\to\infty$*

$$p_2\sim\frac{1}{\gamma^2}. \tag{33}$$

The proof is a special case of Appendix C.

V. n-Copy Frame Error Probability

Consider the channel model presented in Section II. Let p_n denote the frame error probability in a block fading channel assuming that the transmitter sends n copies of

the frame τ seconds apart from each other and an error occurs if and only if all n copies are erroneously decoded.

Lemma 9. *Assume that the fading channel is either Rayleigh or Rician distributed with Gaussian PSD and that a frame error occurs if and only if* $\alpha_i^2(t) \leq \frac{\delta\Omega_p}{\gamma}\ \forall i \in [1,n]$, *where* $\alpha_i(t) = \alpha(t+(i-1)\tau)$. *Then,*

$$p_n = \int_0^{\sqrt{\frac{\delta\Omega_p}{\gamma}}} \overset{(n)}{\cdots} \int_0^{\sqrt{\frac{\delta\Omega_p}{\gamma}}} \int_0^{2\pi} \overset{(n)}{\cdots} \int_0^{2\pi} f_{\boldsymbol{\alpha},\boldsymbol{\theta}}\left(\boldsymbol{\alpha},\boldsymbol{\theta}\right) d\boldsymbol{\theta} d\boldsymbol{\alpha}, \tag{34}$$

where

$$f_{\boldsymbol{\alpha},\boldsymbol{\theta}}\left(\boldsymbol{\alpha},\boldsymbol{\theta}\right) = \frac{\prod_{i=1}^{n}\alpha_i}{(2\pi)^n\sqrt{|\boldsymbol{\Sigma}|}} \exp\left[-\frac{1}{2}\left(\boldsymbol{z}-s\boldsymbol{u}\right)^T \boldsymbol{\Sigma}^{-1}\left(\boldsymbol{z}-s\boldsymbol{u}\right)\right], \tag{35}$$

$$\boldsymbol{z} = \begin{bmatrix}\alpha_1\cos\theta_1 & \alpha_1\sin\theta_1 & \alpha_2\cos\theta_2 & \alpha_2\sin\theta_2 & \cdots & \alpha_n\cos\theta_n & \alpha_n\sin\theta_n\end{bmatrix}^T, \tag{36}$$

$$\boldsymbol{u} = \begin{bmatrix}1 & 0 & \cos\left(\phi_\tau\right) & \sin\left(\phi_\tau\right) & \cdots & \cos\left(n\phi_\tau\right) & \sin\left(n\phi_\tau\right)\end{bmatrix}^T, \tag{37}$$

and $\boldsymbol{\Sigma} \in \mathbb{R}^+_{2n\times 2n}$ *is a symmetric matrix such that*

$$\Sigma_{ij} = \begin{cases} 0 & \text{if } i+j \text{ is odd} \\ b_0 e^{-\frac{1}{2}(\pi|i-j|\tau_n)^2} & \text{if } i+j \text{ is even.}\end{cases} \tag{38}$$

The proof follows directly from extending the results of Appendix B-B to an n-copy transmission scheme.

Lemma 10. *Assume the same transmission scheme as in Lemma 9 and consider a Rayleigh or Rician block fading channel with arbitrary PSD. Then, for all values of* τ, *as* $\gamma \to \infty$,

$$p_n \sim \frac{1}{\gamma^n}. \tag{39}$$

The proof is given in Appendix C.

The result of Lemma 10 is particularly interesting. Indeed, it highlights the fact that even for large SNR conditions, the added benefit (in terms of FER reduction) per extra frame copy sent by the transmitter decreases.[1] Furthermore, this problem is even more notorious at the low SNR regime, where sending multiple copies of a frame results in several errors at the receiver with high probability, thus wasting large amounts of energy (intuitively, if the channel conditions are very bad, the optimal strategy is to pause transmission until the fade event has finished). Therefore, we expect that for practical purposes the number of frame copies sent by the transmitter will be limited to a handful at most.

[1]This can be obtained simply by taking the derivative of Equation 39 with respect to n and noting that it is negative for all $\gamma, n > 0$.

VI. System Model Calibration

Before validating our system model against simulated results, we succinctly summarize how to calibrate its parameter δ. In particular, let $f(\gamma)$ denote the function that returns the FER as a function of $\frac{E_b}{N_0}$ for a given modulation and coding scheme for the AWGN channel.[2] Furthermore, let the frame error rate estimate obtained through numerical integration and through our approximation be defined as follows:

$$FER_1(\gamma) = \int_0^\infty f\left(\alpha^2\gamma\right) p\left(\alpha^2\right) d\alpha^2 \tag{40}$$

$$FER_2(\gamma, \delta) = \int_0^{\sqrt{\frac{\delta\Omega_p}{\gamma}}} p(\alpha) d\alpha. \tag{41}$$

Then, the relative error caused by our ON/OFF approximation for a given γ can be measured as

$$\varepsilon_r(\gamma, \delta) = \frac{FER_2(\gamma, \delta) - FER_1(\gamma)}{FER_1(\gamma)}. \tag{42}$$

Therefore, the optimal choice of δ satisfies

$$\delta^* = \arg\min_\delta \int_0^\infty \varepsilon_r^2(\gamma, \delta)\, d\gamma. \tag{43}$$

To solve this minimization problem we can follow two approaches: On the one hand, this last equation is clearly convex and therefore its minimum can be found by differentiating with respect to δ (assuming that $FER_1(\gamma)$ constant) and equating the resulting expression to zero. Unfortunately, this procedure yields equations that cannot be solved analytically and, consequently, we must rely on numerical methods. Therefore, it is easier to simply obtain δ^* by applying numerical minimization directly to Equation 43.

To exemplify the process of calibration, we consider once again a link where data is first encoded using the CCSDS LDPC with rate 1/2 and 1024 bit frame size, and the modulated using a BPSK modulation. The FER vs. γ curve for the AWGN channel can be obtained from Reference [6], which provides in a finite set of discrete points $(\gamma_i, f(\gamma_i))$ such that $\gamma_i \in [0, 2.5)$ dB. Using these and linear interpolation, we approximate $f(\gamma)$ as a piece-wise linear function and solve Equation 43 using a Matlab's gradient-based optimizer. The results can be observed in Figure 1, which were obtained assuming a Rayleigh fading channel. Note that model calibration for Rician fading channels can be performed following a similar procedure.

Table 1 provides optimal values for δ considering all CCSDS LDPC codes. They are valid for fading channels with $K \in [0, 10]$, and have typical and worst absolute errors

[2]These curves are typically tabulated and can be easily found in the literature. For instance, their values for Turbo and LDPC codes used in the Consultative Committee for Space Data Systems (CCSDS) standards can be found in Reference [6].

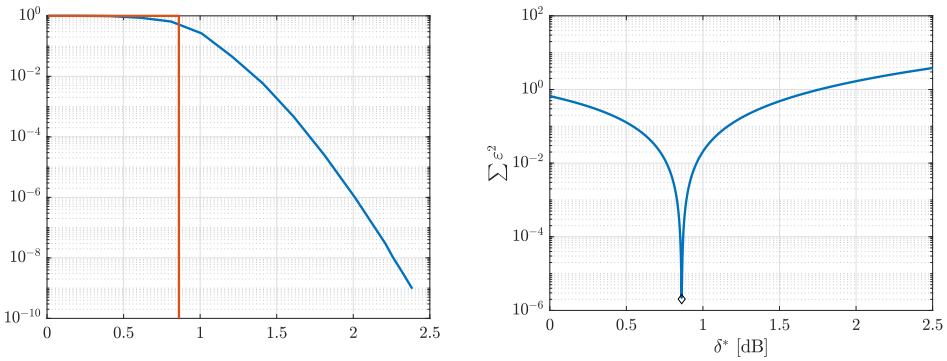

(a) FER vs. E_b/N_0 Curves **(b) Sum of Relative Errors**

Figure 1. Model Calibration Example

Table 1. δ^* for CCSDS LDPC codes

Code Type	Code Rate	Frame Size	δ^* [dB]
LDPC	1/2	1024	0.866
LDPC	2/3	1024	1.636
LDPC	4/5	1024	3.122
LDPC	1/2	4096	0.777
LDPC	2/3	4096	1.550
LDPC	4/5	4096	2.495
LDPC	1/2	16384	0.659
LDPC	2/3	16384	2.100
LDPC	4/5	16384	2.423
LDPC	7/8	7136	4.005

of $\pm$ 0.005 and $\pm$0.25 dB, respectively. Similarly, Figure 2 plots the FER vs. E_b/N_0 curves for four of the CCSDS LDPC codes. Each figure includes three sets of plots:

1. A magenta line showing the code performance over an ideal AWGN channel.
2. A set of colored plots that depict the code performance in a fading channel with given K, computed using Equation 40.
3. A set of black dotted plots that show the same metric estimated using the proposed ON/OFF model (i.e., Equation 41).

Two conclusions are immediate: First, the slow block fading effects largely degrade the code performance when compared to a pure AWGN channel; Second, the proposed ON/OFF model, once properly calibrated, can successfully approximate the FER curves for all considered cases.

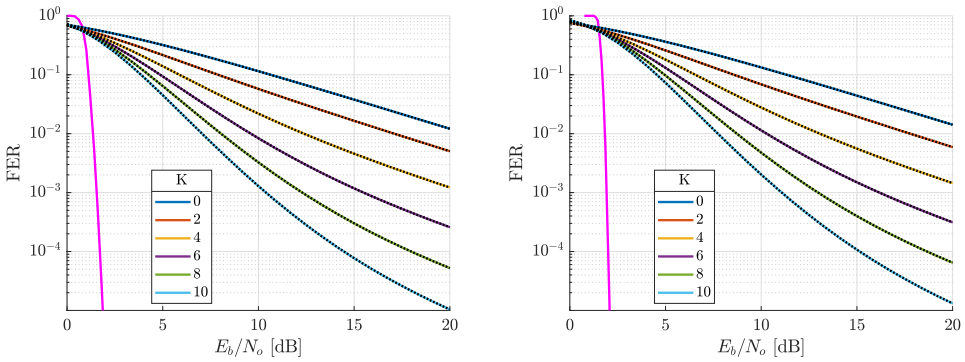

(a) LDPC 1/2 1024 **(b) LDPC 2/3 4096**

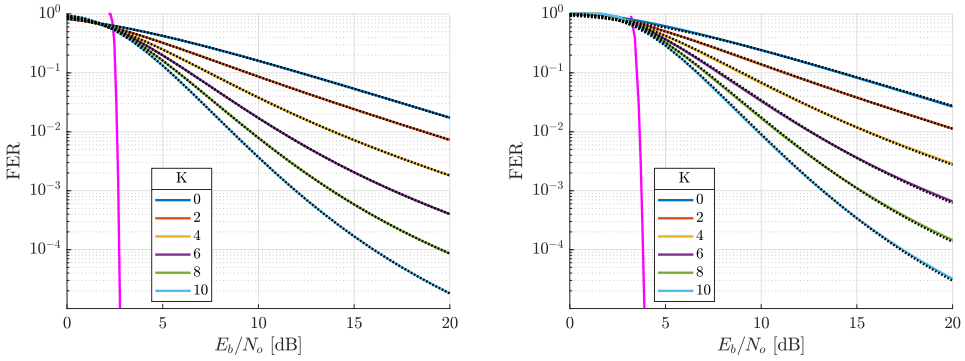

(c) LDPC 4/5 16384 **(d) LDPC 7/8 7136**

Figure 2. Calibrated Models

VII. Numerical Results

A. Dual-Copy System Performance

To exemplify the performance of a dual-copy repetition scheme over a fading-impaired channel, we consider the downlink from the lunar South Pole to a DSN station introduced in Section I. Figure 3 provides the FER vs. E_b/N_0 curves obtained assuming that the fading process has a Gaussian PSD and K equals 0 and 10, respectively. Note that in this case, we provide the system performance with respect to the *information bit* to noise spectral density ratio as discussed in Section II-D.

In Figure 3 we observe that for large E_b/N_0 values, the obtained curves are linear in the logarithmic domain as expected (see Lemma 10). Additionally, for any given E_b/N_0 value, the corresponding FER over the Rician-faded channel is lower than for the Rayleigh-faded channel, as secondary copies arriving at the receiver will have less strength compared to the main line-of-sight (LoS) ray. Furthermore, the gains obtained by sending a dual copy of any given frame are increasingly notable as their time separation increases. Indeed, the difference between waiting for half of the coherence time and a tenth of its value can be more than 10 dB for low frame error rates.

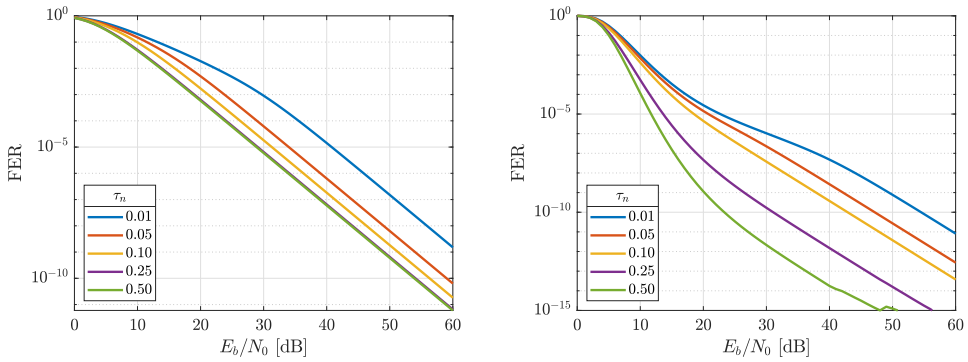

(a) $K = 0$ **(b) $K = 10$**

Figure 3. (Asymptotic) Dual Frame Error Probability vs. (large) E_b/N_0

At this point, it is worth clarifying why separating two copies of a frame by as much as possible is not always beneficial. In particular, as τ_n grows, the second copy of each frame is increasingly delayed, which poses two problems: On the one hand, if the first copy of the frame is lost, the receiver needs to wait for a long period of time before having another chance at getting the data. This is acceptable for delay-tolerant applications like bulk file transfer, but might be problematic for transmitting continuous voice and video streams over channels with large coherence times (as is the case for a downlink from the Moon). On the other hand, the transmitter needs to keep in memory all frames awaiting transmission of their second copy. Therefore, if the incoming data rate is sufficiently large, and the channel fading is sufficiently slow, then the amount of memory required in the spacecraft radio might exceed its technical capabilities. In either case, however, our analysis shows that significant gains in E_b/N_0 can be obtained even if the second copy is sent over channel conditions that are not perfectly independent (e.g., $\tau_n \in [5\%, 25\%]$), especially as fading effects worsen.

B. Single vs. Dual-Copy System Performance

In this section we compare the performance of a dual-copy coded system with a traditional single-copy coded system. Figure 4 plots the obtained results for $K = 0$ and $K = 10$ and provides two sets of curves for each sub-figure. First, a dotted black line that indicates the performance of a single-copy scheme (i.e., p_1 vs. γ). Second, several color-coded curves that indicate the performance of the dual-copy scheme assuming that the second copy is sent after a given normalized delay τ_n (i.e., p_2 vs. γ_2). Results indicate that:

- For very low E_b/N_0 and high FER, the single-copy approach is generally preferable since you are not doubling the amount of data sent over the channel (most of which will be erroneously received anyway).
- At typical mission design values (e.g., FER$= 10^{-4}$), the dual-copy scheme can

improve the overall system performance by several dB. This improvement is increasingly notable as the multi-path fading effects worsen (i.e., for smaller values of K).

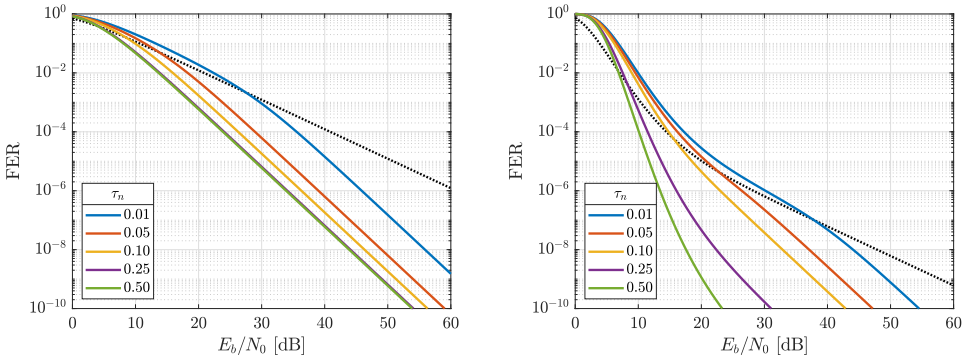

(a) $K = 0$ **(b) $K = 10$**

Figure 4. Dual Frame Error Probability vs. E_b/N_0

Finally, we define the *repetition gap* as the difference in E_b/N_0 between the dual and single-copy schemes, conditional on a fixed FER value.[3] Figure 5 plots the obtained curves for $K = 0$ and $K = 10$ assuming that $\tau_n \geq 0.5$. Note that negative values of the repetition gap indicate that the dual-copy scheme performs worse than the traditional single-copy approach and, consequently, it should not be utilized (and vice versa). On the other hand, for FER=10^{-5}, we conclude that missions affected by a multi-path fading effects can improve their link performance by approximately 4 to 17 dB. Finally, note also that for large SNR values (or low FER), the repetition gap increases linearly in the logarithmic scale, an expected behavior given our asymptotic calculations.[4]

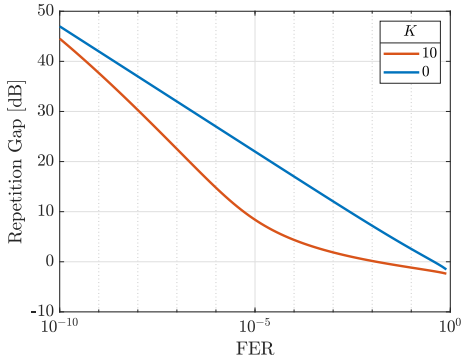

Figure 5. Repetition Gap vs. Frame Error Probability

[3]This figure of merit is analogous to the coding gap, but using p_1 as a reference point.

[4]In reality the repetition gap would be limited by the LDPC error floor, which we have ignored in the proposed channel model.

VIII. Conclusions

This paper considers the problem of estimating the frame error probability in a frequency-flat, slow-varying channel experiencing Rayleigh or Rician block fading. To that end, we consider a system model in which the receiver has perfect timing and synchronization and show that, after calibration, the overall system can be modeled as an ON/OFF channel where frames are lost if the fade-level exceeds a certain threshold. Using this model, we then derive analytic or semi-analytic expressions for the single and dual-frame error probability, where the latter indicates the probability of not receiving a frame for which a second copy is transmitted τ seconds apart. Furthermore, we generalize these results to an n-copy transmission scheme and provide asymptotic behavior of the frame error rate under large signal-to-noise ratio conditions.

To exemplify the usefulness of combined repetition and forward error correction schemes in the presence of fading, we compare the end-to-end system performance with and without frame repetition for a link between the lunar South Pole and a DSN station. We show that for typical FER values, a dual-copy repetition scheme results in E_b/N_0 savings between 4 and 17 dB, depending on the severity of the multi-path fading effects and assuming no interleaving is used at the transmitter and receiver. Therefore, this hybrid scheme can be useful in situations where slow fading prevents the use of interleaving due to memory and/or latency considerations.

IX. Acknowledgments

The author would like to acknowledge David Heckman, Kar-Ming Cheung, and Norman Lay, from the Jet Propulsion Laboratory, for their help simplifying some of the integrals in this paper and reviewing it. The author would also like to acknowledge Dariush Divsalar and Ken Andrews, also from the Jet Propulsion Laboratory, for their help with estimating the performance of the CCSDS LDPC codes. Finally, the author would like to acknowledge Mary Young for the editorial comments. NASA sponsorship through the Space Communication and Navigation Program (SCaN) is also acknowledged.

Appendices

I. Frame Error Probability

A. Rayleigh Fading

To compute the FER over a Rayleigh channel experiencing block fading we simply integrate its envelope's probability density distribution:

$$p_1 = \int_0^{\sqrt{\delta\Omega_p/\gamma}} \frac{\alpha}{b_0} e^{-\frac{\alpha^2}{2b_0}} d\alpha = 1 - e^{-\frac{\delta\Omega_p/\gamma}{2b_0}} = 1 - e^{-\frac{\delta}{\gamma}} \tag{44}$$

B. Rician Fading

To compute the FER over a Rician channel experiencing block fading we integrate its envelope's probability density distribution and utilize the following change of variables: $u = \frac{\alpha}{\sqrt{b_0}}$. Then,

$$\begin{aligned} p_1 = & \int_0^{\sqrt{\delta\Omega_p/\gamma}} \frac{\alpha}{b_0} e^{-\frac{\alpha^2+s^2}{2b_0}} I_0\left(\frac{\alpha s}{b_0}\right) d\alpha = \\ = & \int_0^{\sqrt{2(K+1)\frac{\delta}{\gamma}}} u e^{-\frac{u^2+2K}{2}} I_0\left(\sqrt{2K}u\right) du = \\ = & 1 - Q\left(\sqrt{2K}, \sqrt{2(K+1)\frac{\delta}{\gamma}}\right) \end{aligned} \tag{45}$$

II. Dual Frame Error Probability

A. Rayleigh Fading

Given the channel and receiver model described in Section II, the error probability of a segment sent twice τ seconds apart can be simply estimated as

$$p_2 = \mathrm{P}\left(\alpha_1 \leq \sqrt{\frac{\delta\Omega_p}{\gamma}}, \alpha_2 \leq \sqrt{\frac{\delta\Omega_p}{\gamma}}\right). \tag{46}$$

Lemma 4 provides a generic formula to evaluate this joint probability as a function of the channel PSD. In particular,

$$\mu_1 = \int_{-\infty}^{\infty} S(f)\cos(2\pi f\tau)\, df = \int_0^{\infty} \frac{2b_0}{\sqrt{2\pi}\sigma_f} e^{-\frac{f^2}{2\sigma_f^2}} \cos(2\pi f\tau)\, df = b_0\rho(\tau_n), \tag{47}$$

where $\tau_n = \sigma_f\tau = \frac{\tau}{T_c}$ denotes the normalized delay and $\rho(\tau_n) = e^{-2(\pi\tau_n)^2}$ denotes the normalized autocorrelation between the envelope level at two instants in time

separated by τ seconds (see Figure 6). Note that this autocorrelation decays exponentially with the square of the normalized delay and is negligible for all values $\tau_n \geq 0.5$. In other words, in a flat-fading channel characterized by a Gaussian PSD, you only need to wait half of the coherence time to obtain independent channel realizations.

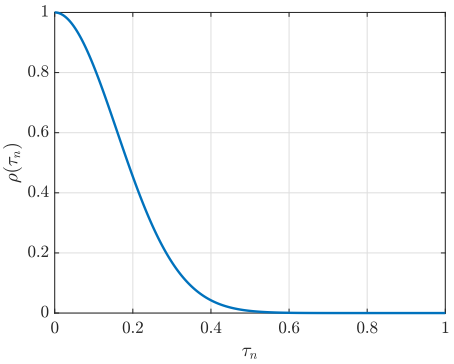

Figure 6. Correlation of the Fading Envelope

On the other hand,

$$\mu_2 = \int_{-\infty}^{\infty} S(f) \sin\left(2\pi\left(f - f_0\right)\tau\right) df = 0 \tag{48}$$

since the integrand is an odd function and the integration domain is symmetric with respect to 0. Therefore,

$$A = b_0^2 - \gamma_1^2 - \gamma_2^2 = b_0^2\left[1 - e^{-(2\pi\tau_n)^2}\right] = b_0\left[1 - \rho^2\right]. \tag{49}$$

To obtain p_2, we simply substitute the obtained values for μ_1 and μ_2 into Equation 16. This yields

$$\begin{aligned} p_2 &= \int_0^{\sqrt{\delta\Omega_p/\gamma}} \int_0^{\sqrt{\delta\Omega_p/\gamma}} \frac{\alpha_1\alpha_2}{A} e^{-\frac{b_0}{2A}\left(\alpha_1^2+\alpha_2^2\right)} I_0\left(\frac{\alpha_1\alpha_2}{A} b_0\rho\right) d\alpha_1 d\alpha_2 \\ &= \int_0^{\sqrt{\delta\Omega_p/\gamma}} \frac{\alpha_1}{A} e^{-\frac{b_0}{2A}\alpha_1^2} \int_0^{\sqrt{\delta\Omega_p/\gamma}} \alpha_2 e^{-\frac{b_0}{2A}\alpha_2^2} I_0\left(\frac{\alpha_1\alpha_2}{A} b_0\rho\right) d\alpha_2 d\alpha_1. \end{aligned} \tag{50}$$

We now introduce the following change of variables: $u = \sqrt{\frac{b_0}{A}}\alpha_2$. Then, after some simplification we get

$$p_2 = \int_0^{\sqrt{\delta\Omega_p/\gamma}} \frac{\alpha_1}{b_0} e^{-\frac{b_0}{2A}\alpha_1^2} \int_0^{\sqrt{\frac{2}{1-\rho^2}\frac{\delta}{\gamma}}} u e^{-\frac{u^2}{2}} I_0\left(\sqrt{\frac{b_0}{A}}\rho\alpha_1 u\right) du d\alpha_1. \tag{51}$$

Let us now define $s = \sqrt{\frac{b_0}{A}}\rho\alpha_1$. Then,

$$\begin{aligned} p_2 &= \int_0^{\sqrt{\delta\Omega_p/\gamma}} \frac{\alpha_1}{b_0} e^{-\frac{b_0}{2A}\alpha_1^2} e^{\frac{s^2}{2}} \int_0^{\sqrt{\frac{2}{1-\rho^2}\frac{\delta}{\gamma}}} u e^{-\frac{u^2+s^2}{2}} I_0(su)\, du d\alpha_1 \\ &= \int_0^{\sqrt{\delta\Omega_p/\gamma}} \frac{\alpha_1}{b_0} e^{-\frac{b_0}{2A}\left[1-\rho^2\right]\alpha_1^2} \left[Q(s,0) - Q\left(s, \sqrt{\frac{2}{1-\rho^2}\frac{\delta}{\gamma}}\right)\right]. \end{aligned} \tag{52}$$

Next, we note that $Q(s,0) = 1\ \forall s$ and therefore,

$$p_2 = p_1 - \int_0^{\sqrt{\delta\Omega_p/\gamma}} \frac{\alpha_1}{b_0} e^{-\frac{\alpha_1^2}{2b_0}} Q(s,z)\, d\alpha_1, \tag{53}$$

where $z = \sqrt{\frac{2}{1-\rho^2}\frac{\delta}{\gamma}}$. Therefore, concentrate our attention on this new integral:

$$\int_0^{\sqrt{\delta\Omega_p/\gamma}} \frac{\alpha_1}{b_0} e^{-\frac{\alpha_1^2}{2b_0}} Q(s,z)\, d\alpha_1 = \int_0^{\infty} \frac{\alpha_1}{b_0} e^{-\frac{\alpha_1^2}{2b_0}} Q(s,z)\, d\alpha_1 - \int_{\sqrt{\delta\Omega_p/\gamma}}^{\infty} \frac{\alpha_1}{b_0} e^{-\frac{\alpha_1^2}{2b_0}} Q(s,z)\, d\alpha_1. \tag{54}$$

The first term of the right-hand side of this equation can be shown to be equal to $e^{-\frac{\delta}{\gamma}}$ using Equation (12) of Reference [7]. Similarly, using Equation (14) of this same reference results in

$$\int_{\sqrt{\delta\Omega_p/\gamma}}^{\infty} \frac{\alpha_1}{b_0} e^{-\frac{\alpha_1^2}{2b_0}} Q(s,z)\, d\alpha_1 = e^{-\frac{\delta}{\gamma}} \left[1 + Q(z\rho, z) - Q(z, z\rho)\right]. \tag{55}$$

Finally, assume that $\tau_n \geq 0.5$ so that $\mu_1 \approx 0$ and $A \approx b_0^2$. Then,

$$\begin{aligned} \mathrm{P}\left(\alpha_1 \leq \sqrt{\tfrac{\delta\Omega_p}{\gamma}}, \alpha_2 \leq \sqrt{\tfrac{\delta\Omega_p}{\gamma}}\right) &\approx \int_0^{\sqrt{\delta\Omega_p/\gamma}} \int_0^{\sqrt{\delta\Omega_p/\gamma}} \frac{\alpha_1\alpha_2}{A} e^{-\frac{b_0}{2A}\left(\alpha_1^2+\alpha_2^2\right)} I_0(0)\, d\alpha_1 d\alpha_2 \\ &= \int_0^{\sqrt{\delta\Omega_p/\gamma}} \frac{\alpha_1}{b_0} e^{-\frac{b_0}{2A}\alpha_1^2} d\alpha_1 \int_0^{\sqrt{\delta\Omega_p/\gamma}} \frac{\alpha_2}{b_0} e^{-\frac{b_0}{2A}\alpha_2^2} d\alpha_2 \\ &= \mathrm{P}\left(\alpha(t) \leq \sqrt{\tfrac{\delta\Omega_p}{\gamma}}\right) \mathrm{P}\left(\alpha(t+\tau) \leq \sqrt{\tfrac{\delta\Omega_p}{\gamma}}\right) \\ &= \left[1 - e^{-\frac{\delta}{\gamma}}\right]^2 \end{aligned} \tag{56}$$

B. Rician Fading

We wish to estimate the probability that the signal envelope $\alpha(t)$ falls below a certain threshold $\sqrt{\frac{\delta\Omega_p}{\gamma}}$ at two instants in time separated by τ seconds. Let $\alpha_1 = \alpha(t)$ and

$\alpha_2 = \alpha(t+\tau)$ and consider the case that the transmitters sends an unmodulated tone at the carrier frequency. Then, from Section II-B, we know that we can express the complex baseband equivalent of the received signal as

$$r(t) = [s + N_I(t)] + jN_Q(t) \tag{57}$$

$$r(t+\tau) = [s\cos(2\pi f_c\tau) + N_I(t)] + j[s\sin(2\pi f_c\tau) + N_Q(t)], \tag{58}$$

where

$$N_I(t) \sim \mathcal{N}(0, b_0) \tag{59}$$

$$N_Q(t) \sim \mathcal{N}(0, b_0). \tag{60}$$

Let $x_1 = N_I(t)$, $y_1 = N_Q(t)$, $x_2 = N_I(t+\tau)$ and $y_2 = N_Q(t+\tau)$, and define the column vector $\boldsymbol{r} = \begin{bmatrix} x_1 & y_1 & x_2 & y_2 \end{bmatrix}^T$. Then, $r(t)$ and $r(t+\tau)$ are jointly distributed according to a multivariate normal distribution such that

$$f_{\boldsymbol{r}}(\boldsymbol{r}) = \frac{1}{(2\pi)^2\sqrt{|\boldsymbol{\Sigma}|}} \exp\left[-\frac{1}{2}\boldsymbol{r}^T\boldsymbol{\Sigma}^{-1}\boldsymbol{r}\right] \tag{61}$$

where

$$\boldsymbol{\Sigma} = \begin{bmatrix} b_0 & 0 & \mu_1 & \mu_2 \\ 0 & b_0 & -\mu_2 & \mu_1 \\ \mu_1 & -\mu_2 & b_0 & 0 \\ \mu_2 & \mu_1 & 0 & b_0 \end{bmatrix}, \tag{62}$$

$\phi_\tau = 2\pi f_c\tau$ and

$$\mu_1 = \langle x_1 x_2 \rangle = \langle y_1 y_2 \rangle = \int_{-\infty}^{\infty} S(f)\cos(2\pi(f - f_0)\tau)\, df \tag{63}$$

$$\mu_2 = \langle x_1 y_2 \rangle = -\langle x_2 y_1 \rangle = \int_{-\infty}^{\infty} S(f)\sin(2\pi(f - f_0)\tau)\, df. \tag{64}$$

Note that $\langle\cdot\rangle$ is used here to denote the expectation operator. Note also that if $s = 0$, then these results equate to Lemma 4.

To compute the distribution of the signal envelope $\alpha(t)$ we first apply the following change of variables

$$\alpha_1\cos\theta_1 = s + x_1 \tag{65}$$

$$\alpha_1\sin\theta_1 = y_1 \tag{66}$$

$$\alpha_2\cos\theta_2 = s\cos\phi_\tau + x_2 \tag{67}$$

$$\alpha_2\sin\theta_2 = s\sin\phi_\tau + y_2, \tag{68}$$

and then integrate the resulting joint distribution with respect to θ_1 and θ_2. In other

words, define

$$\boldsymbol{e} = \begin{bmatrix} \alpha_1 \cos\theta_1 \\ \alpha_1 \sin\theta_1 \\ \alpha_2 \cos\theta_2 \\ \alpha_2 \sin\theta_2 \end{bmatrix}, \quad \boldsymbol{u} = \begin{bmatrix} s \\ 0 \\ s\cos\phi_\tau \\ s\sin\phi_\tau \end{bmatrix}. \tag{69}$$

Then,

$$f_{\boldsymbol{\alpha},\boldsymbol{\theta}}(\alpha_1,\alpha_2,\theta_1,\theta_2) = \frac{\alpha_1\alpha_2}{(2\pi)^2\sqrt{|\boldsymbol{\Sigma}|}} \exp\left[-\frac{1}{2}(\boldsymbol{e}-\boldsymbol{u})^T \boldsymbol{\Sigma}^{-1}(\boldsymbol{e}-\boldsymbol{u})\right] \tag{70}$$

and, therefore,

$$f_{\boldsymbol{\alpha}}(\alpha_1,\alpha_2) = \int_0^{2\pi}\int_0^{2\pi} f_{\boldsymbol{\alpha},\boldsymbol{\theta}}(\alpha_1,\alpha_2,\theta_1,\theta_2)\, d\theta_1 d\theta_2. \tag{71}$$

Note that while performing the change of variables we have used the fact that $|f_{\boldsymbol{r}}(\boldsymbol{r})\, d\boldsymbol{r}| = |f_{\boldsymbol{\alpha},\boldsymbol{\theta}}(\boldsymbol{\alpha},\boldsymbol{\theta})\, d\boldsymbol{\alpha} d\boldsymbol{\theta}|$.

Finally, expanding the term $(\boldsymbol{r}-\boldsymbol{u})^T \boldsymbol{\Sigma}^{-1}(\boldsymbol{r}-\boldsymbol{u})$ and simplifying the corresponding equation yields the result from Lemma 6.

C. Rician Fading with Gaussian PSD

If we assume the channel is Rician and characterized by a Gaussian PSD, then further simplifications are possible. In particular,

$$f_{\boldsymbol{\alpha}}(\alpha_1,\alpha_2) = \frac{\alpha_1\alpha_2}{(2\pi)^2 A} e^{-\frac{b_0}{2A}(z_1 - 2s^2 z_5)} \int_0^{2\pi}\left[g_1(z_2) \int_0^{2\pi} g_2(z_3,z_4)\, d\theta_2 \right] d\theta_1 \tag{72}$$

where

$$z_1 = \alpha_1^2 + \alpha_2^2 \tag{73}$$

$$z_2 = \rho\cos(\theta_1 - \phi_\tau) - \cos\theta_1 \tag{74}$$

$$z_3 = \rho\cos\theta_2 - \cos(\theta_2 - \phi_\tau) \tag{75}$$

$$z_4 = \rho\cos(\theta_1 - \theta_2) \tag{76}$$

$$z_5 = \rho\cos\phi_\tau - 1 \tag{77}$$

and ϕ_τ is defined as before. Expanding all terms in $g_2(z_3,z_4)$ and grouping them in terms of $\cos\theta_2$ and $\sin\theta_2$ yields

$$\int_0^{2\pi} g_2(z_3,z_4)\, d\theta_2 = \int_0^{2\pi} e^{x_1\cos\theta_2 + x_2\sin\theta_2} d\theta_2 = 2\pi I_0\left(\sqrt{x_1^2+x_2^2}\right), \tag{78}$$

where

$$x_1 = \frac{s b_0 \alpha_2}{A}\left[\cos\phi_\tau + \rho\left(\frac{\alpha_1}{s}\cos\theta_1 - 1\right)\right] \tag{79}$$

$$x_2 = \frac{s b_0 \alpha_2}{A}\left[\sin\phi_\tau + \frac{\alpha_1}{s}\rho\sin\theta_1\right]. \tag{80}$$

Therefore,

$$f_{\boldsymbol{\alpha}}\left(\alpha_1,\alpha_2\right)=\frac{\alpha_1\alpha_2}{2\pi A}e^{-\frac{b_0}{2A}\left(z_1-2s^2z_5\right)}\int_0^{2\pi}g_1\left(z_2\right)I_0\left(\sqrt{x_1^2+x_2^2}\right)d\theta_1, \tag{81}$$

which, after some simplification, yields

$$f_{\boldsymbol{\alpha}}\left(\alpha_1,\alpha_2\right)=\frac{\alpha_1\alpha_2}{2\pi A}e^{-\frac{b_0}{2A}\left[\alpha_1^2+\alpha_2^2-2s^2B\right]}\int_0^{2\pi}e^{-\frac{\alpha_1 sb_0}{A}\left[B\cos\theta_1+C\sin\theta_1\right]}I_0\left(D\alpha_2\right)d\theta_1, \tag{82}$$

and

$$A=b_0^2\left[1-\rho^2\right] \tag{83}$$

$$B=\rho\cos\phi_\tau-1 \tag{84}$$

$$C=\rho\sin\phi_\tau \tag{85}$$

$$D=\frac{sb_0}{A}\sqrt{1+\rho^2y_1+2\rho y_2} \tag{86}$$

$$y_1=\left(\frac{\alpha_1}{s}\right)^2-\frac{2\alpha_1}{s}\cos\theta_1+1 \tag{87}$$

$$y_2=\frac{\alpha_1}{s}\cos\left(\theta_1-\phi_\tau\right)-\cos\phi_\tau. \tag{88}$$

Next, we modify the integration order so that

$$p_2=\int_0^{\sqrt{\delta\Omega_p/\gamma}}\int_0^{2\pi}\frac{\alpha_1}{2\pi}e^{-\frac{b_0}{2A}\left[\alpha_1^2-2s^2B\right]-\frac{\alpha_1 sb_0}{A}\left[B\cos\theta_1+C\sin\theta_1\right]}\Upsilon\left(\alpha_1,\theta_1\right)d\theta_1d\alpha_1, \tag{89}$$

where

$$\Upsilon\left(\alpha_1,\theta_1\right)=\int_0^{\sqrt{\delta\Omega_p/\gamma}}\frac{\alpha_2}{A}e^{-\frac{b_0}{2A}\alpha_2^2}I_0\left(D\alpha_2\right)d\alpha_2 \tag{90}$$

and we then concentrate our attention on this new integral, which we solve using the change of variables $u=\sqrt{\frac{b_0}{A}}\alpha_2$:

$$\begin{aligned}\Upsilon\left(\alpha_1,\theta_1\right)=&\int_0^{\infty}\frac{u}{b_0}e^{-\frac{u^2}{2}}I_0\left(zu\right)du-\int_{\sqrt{\frac{2(K+1)}{1-\rho^2}\frac{\delta}{\gamma}}}^{\infty}\frac{u}{b_0}e^{-\frac{u^2}{2}}I_0\left(zu\right)du\\=&\frac{e^{\frac{z^2}{2}}}{b_0}\left[\int_0^{\infty}\frac{u}{b_0}e^{-\frac{u^2+z^2}{2}}I_0\left(zu\right)du-\int_{\sqrt{\frac{2(K+1)}{1-\rho^2}\frac{\delta}{\gamma}}}^{\infty}\frac{u}{b_0}e^{-\frac{u^2+z^2}{2}}I_0\left(zu\right)du\right]\\=&\frac{e^{\frac{z^2}{2}}}{b_0}\left[1-Q\left(z,\sqrt{\frac{2(K+1)}{1-\rho^2}\frac{\delta}{\gamma}}\right)\right],\end{aligned} \tag{91}$$

with $z = \sqrt{2K\frac{1+\rho^2 y_1 + 2\rho y_2}{1-\rho^2}}$.

At this point, we need to evaluate the two parts of this result separately. Therefore, we first solve

$$\begin{aligned}
&\int_0^{\sqrt{\delta\Omega_p/\gamma}} \frac{\alpha_1}{2\pi b_0} e^{-\frac{b_0}{2A}\left[\alpha_1^2 - 2s^2 B\right]} \int_0^{2\pi} e^{\frac{z^2}{2} - \frac{\alpha_1 s b_0}{A}[B\cos\theta_1 + C\sin\theta_1]} d\theta_1 d\alpha_1 = \\
&\int_0^{\sqrt{\delta\Omega_p/\gamma}} \frac{\alpha_1}{2\pi b_0} e^{-\frac{b_0}{2A}\left[\alpha_1^2 - 2s^2 B\right]} e^{x_1} \int_0^{2\pi} e^{x_2\cos\theta_1} d\theta_1 d\alpha_1 = \\
&\int_0^{\sqrt{\delta\Omega_p/\gamma}} \frac{\alpha_1}{b_0} e^{-\frac{b_0}{2A}\left[\alpha_1^2 - 2s^2 B\right] + x_1} I_0\left(\tfrac{s\alpha_1}{b_0}\right) d\alpha_1 = \\
&\int_0^{\sqrt{\delta\Omega_p/\gamma}} \frac{\alpha_1}{b_0} e^{-\frac{\alpha_1^2 + s^2}{2b_0}} I_0\left(\tfrac{s\alpha_1}{b_0}\right) d\alpha_1 = 1 - Q\left(\sqrt{2K}, 2(K+1)\sqrt{\tfrac{\delta}{\gamma}}\right) = p_1
\end{aligned} \tag{92}$$

using

$$x_1 = \frac{\rho^2}{2b_0(1-\rho^2)}\alpha_1^2 + K\frac{1+\rho^2 - 2\rho\cos\phi_\tau}{1-\rho^2} \tag{93}$$

$$x_2 = \frac{s}{b_0}\alpha_1, \tag{94}$$

and the fact that the very last expression has already been solved in Appendix A-B. Therefore, at this point we have proven that

$$p_2 = p_1 - \int_0^{\sqrt{\delta\Omega_p/\gamma}} \int_0^{2\pi} \frac{\alpha_1}{2\pi b_0} e^{-\frac{b_0}{2A}\left[\alpha_1^2 - 2s^2 B\right] + x_1 + x_2\cos\theta_1} Q\left(z, \sqrt{\tfrac{2(K+1)}{(1-\rho^2)}\tfrac{\delta}{\gamma}}\right) d\theta_1 d\alpha_1, \tag{95}$$

which, after some simplification, yields the result in Lemma 7.

D. Independent Rician Fading with Gaussian PSD

We now consider the case that $\tau_n \geq 0$ so that $\rho \approx 0$. Then, $x_1 \approx K$, $z \approx \sqrt{2K}$, and $B \approx -1$, which yields

$$\begin{aligned}
p_2 \approx & p_1 - \int_0^{\sqrt{\delta\Omega_p/\gamma}} \int_0^{2\pi} \frac{\alpha_1}{2\pi b_0} e^{-\frac{b_0}{2A}\left[\alpha_1^2+2s^2\right]+\frac{s^2}{2b_0}+x_2\cos\theta_1} Q\left(\sqrt{2K}, \sqrt{\tfrac{2(K+1)}{(1-\rho^2)}\tfrac{\delta}{\gamma}}\right) d\theta_1 d\alpha_1 \\
= & p_1 - Q\left(\sqrt{2K}, \sqrt{\tfrac{2(K+1)}{(1-\rho^2)}\tfrac{\delta}{\gamma}}\right) \int_0^{\sqrt{\delta\Omega_p/\gamma}} \frac{\alpha_1}{2\pi b_0} e^{-\frac{b_0}{2A}\left[\alpha_1^2+s^2\right]} \int_0^{2\pi} e^{x_2\cos\theta_1} d\theta_1 d\alpha_1 \\
= & p_1 - Q\left(\sqrt{2K}, \sqrt{\tfrac{2(K+1)}{(1-\rho^2)}\tfrac{\delta}{\gamma}}\right) \int_0^{\sqrt{\delta\Omega_p/\gamma}} \frac{\alpha_1}{2\pi b_0} e^{-\frac{b_0}{2A}\left[\alpha_1^2+s^2\right]} I_0\left(\tfrac{s\alpha_1}{b_0}\right) d\alpha_1 \\
= & p_1 - Q\left(\sqrt{2K}, \sqrt{\tfrac{2(K+1)}{(1-\rho^2)}\tfrac{\delta}{\gamma}}\right)\left[1 - Q\left(\sqrt{2K}, \sqrt{\tfrac{2(K+1)}{(1-\rho^2)}\tfrac{\delta}{\gamma}}\right)\right] \\
= & \left[1 - Q\left(\sqrt{2K}, \sqrt{2(K+1)\tfrac{\delta}{\gamma}}\right)\right]^2 = p_1^2.
\end{aligned} \tag{96}$$

Note that this confirms the intuition that two channel realizations far apart will be independent from each other and therefore the joint loss probability is simply the product of the marginal probabilities.

III. Asymptotic Behavior

To obtain the asymptotic behavior of p_n when $\gamma \to \infty$ we use the following procedure: First we obtain the derivative of p_n with respect to γ. Then, we find the asymptotic behavior of that derivative for $\gamma \to \infty$. Finally, we integrate the result to obtain the asymptotic behavior of p_n.

Before proceeding with the proof, we define a few of its building blocks. For instance, let $f(x,t)$ be a continuous differentiable function. Then, the Leibniz rule of differentiation states that

$$\frac{\partial}{\partial x}\left(\int_{a(x)}^{b(x)} f(x,t)dt\right) = f\left(x,b(x)\right)\frac{\partial b(x)}{\partial x} - f\left(x,a(x)\right)\frac{\partial a(x)}{\partial x} + \int_{a(x)}^{b(x)} \frac{\partial}{\partial x} f(x,t)dt. \tag{97}$$

Similarly, let us also define the following function:

$$h_k\left(\gamma,\alpha_k\right) = \int_0^{\sqrt{\frac{\delta\Omega_p}{\gamma}}} \overset{(n-k)}{\cdots} \int_0^{\sqrt{\frac{\delta\Omega_p}{\gamma}}} \int_0^{2\pi} \overset{(n)}{\cdots} \int_0^{2\pi} \left[\prod_{i=1}^{n} \alpha_i e^{-\frac{1}{2}\boldsymbol{z}^T\boldsymbol{\Sigma}^{-1}\boldsymbol{z}}\right] d\boldsymbol{\theta} \prod_{i>k}^{n} d\alpha_i, \tag{98}$$

where $\boldsymbol{z} = \boldsymbol{e} - s\boldsymbol{u}$, $\boldsymbol{e}$ and $\boldsymbol{u}$ are defined as in Lemma 9. Then, we note the following properties:

$$p_n = \frac{h_0(\gamma)}{(2\pi)^n \sqrt{|\boldsymbol{\Sigma}|}} = \frac{1}{(2\pi)^n \sqrt{|\boldsymbol{\Sigma}|}} \int_0^{\sqrt{\frac{\delta\Omega_p}{\gamma}}} h_1(\gamma, \alpha_1)\, d\alpha_1, \tag{99}$$

$$h_k(\gamma, \alpha_k) = \int_0^{\sqrt{\frac{\delta\Omega_p}{\gamma}}} h_{k+1}(\gamma, \alpha_{k+1}) d\alpha_{k+1} \tag{100}$$

$$\frac{\partial}{\partial\gamma} h_k(\gamma, \alpha_k) \propto \begin{cases} \frac{1}{\gamma^{\frac{3}{2}}} h_{k+1}\Big(\gamma, \alpha_{k+1}{=}\sqrt{\frac{\delta\Omega_p}{\gamma}}\Big) + \int_0^{\sqrt{\frac{\delta\Omega_p}{\gamma}}} \frac{\partial}{\partial\gamma} h_{k+1}(\gamma, \alpha_{k+1})\, \alpha_{k+1} & \text{if } k \in [1, n-1] \\ 0 & \text{if } k = n, \end{cases} \tag{101}$$

$$\begin{aligned} \frac{1}{\gamma^{\frac{3}{2}}} h_{k+1}\left(\gamma, \alpha_{k+1}{=}\sqrt{\frac{\delta\Omega_p}{\gamma}}\right) &= \int_0^{\sqrt{\frac{\delta\Omega_p}{\gamma}}} \overset{(n-k-1)}{\cdots} \int_0^{\sqrt{\frac{\delta\Omega_p}{\gamma}}} \int_0^{2\pi} \overset{(n)}{\cdots} \int_0^{2\pi} \prod_{i\neq k+1}^{n} \alpha e^{-\frac{1}{2}\boldsymbol{z}^T\boldsymbol{\Sigma}^{-1}\boldsymbol{z}} d\boldsymbol{\theta} \prod_{i>k}^{n} d\alpha_i \\ &\propto \frac{1}{\gamma^{\frac{3}{2}}} \frac{1}{\gamma^{\frac{1}{2}}} \left[\prod_{i=1}^{k} \alpha_i\right] \prod_{i=k+1}^{n} \left[\int_0^{\sqrt{\frac{\delta\Omega_p}{\gamma}}} \alpha_i d\alpha_i\right] \\ &\propto \frac{1}{\gamma^{n-k+1}} \prod_{i=1}^{k} \alpha_i. \end{aligned} \tag{102}$$

Equation 102 is only valid for $\gamma \to \infty$ since we have used the fact that

$$e^{-\frac{1}{2}\boldsymbol{z}^T\boldsymbol{\Sigma}^{-1}\boldsymbol{z}} \sim 1 + o\left(\tfrac{1}{\sqrt{\gamma}}\right) \tag{103}$$

when $\boldsymbol{z}^T\boldsymbol{\Sigma}^{-1}\boldsymbol{z}$ is evaluated at

$$\boldsymbol{z} = \left[\alpha_1\cos\theta_1 \quad \alpha_1\sin\theta_1 \quad \cdots \quad \sqrt{\tfrac{\delta\Omega_p}{\gamma}}\cos\theta_{k+1} \quad \sqrt{\tfrac{\delta\Omega_p}{\gamma}}\sin\theta_{k+1} \quad \cdots \quad \alpha_n\cos\theta_n \quad \alpha_n\sin\theta_n\right]. \tag{104}$$

Combining Equations 101 and 102 for $k = n-1$ yields

$$\frac{\partial}{\partial\gamma} h_{n-1}(\gamma, \alpha_{n-1}) \propto \frac{1}{\gamma^2} \prod_{i=1}^{n-1} \alpha_i + 0. \tag{105}$$

This value can now be used recursively to evaluate $h_{n-2}(\gamma, \alpha_{n-2})$ and its predecessors. For instance,

$$\frac{\partial}{\partial\gamma} h_{n-2}(\gamma, \alpha_{n-2}) \propto \frac{1}{\gamma^3} \prod_{i=1}^{n-2} \alpha_i + \frac{1}{\gamma^2} \prod_{i=1}^{n-2} \alpha_i \int_0^{\sqrt{\frac{\delta\Omega_p}{\gamma}}} \alpha_{n-1} d\alpha_{n-1} \propto \frac{1}{\gamma^3} \prod_{i=1}^{n-2} \alpha_i \tag{106}$$

and, therefore, we obtain the following general expression:

$$\frac{\partial}{\partial\gamma}h_k\left(\gamma,\alpha_k\right) \propto \frac{1}{\gamma^{n-k+1}}\prod_{i=1}^{k}\alpha_i. \tag{107}$$

Finally, we recall that p_n is proportional to $h_k\left(\gamma,\alpha_k\right)$ when $k=0$. Therefore,

$$\frac{\partial}{\partial\gamma}p_n \propto \frac{1}{\gamma^{n+1}} \tag{108}$$

and, consequently,

$$p_n \propto \int \frac{1}{\gamma^{n+1}} \propto \frac{1}{\gamma^n}. \tag{109}$$

References

[1] M. Sanchez Net, "Analysis of the Fading Channel in Downlinks from the Lunar South Pole to the Deep Space Network," *The Interplanetary Network Progress Report*, vol. 42-216, pp. 1–30, February 2019. https://ipnpr.jpl.nasa.gov/progress_report/42-216/42-216C.pdf

[2] R. G. Gallager, *Information theory and reliable communication*. Wiley, 1968, vol. 2.

[3] D. Divsalar, M. Sanchez Net, and K. Cheung, "Acquisition and Tracking for Communications Between the Lunar South Pole and Earth," in *Aerospace Conference, 2019. Proceedings. 2019 IEEE*. IEEE, 2019.

[4] G. Matz and F. Hlawatsch, "Fundamentals of Time-Varying Communication Channels," in *Wireless Communications over Rapidly Time-Varying Channels*. Academic Press, 2011, pp. 1–63.

[5] S. O. Rice, "Mathematical Analysis of Random Noise," *Bell System Technical Journal*, vol. 23, no. 3, pp. 282–332, July 1944.

[6] Consultative Committee for Space Data Systems, "TM Synchronization and Channel Coding - Summary of Concept and Rationale," Consultative Committee for Space Data Systems, Tech. Rep. CCSDS 130.1-G-2, November 2012.

[7] A. Nuttall, "Some Integrals Involving the Q_M Function," *IEEE Transactions on Information Theory*, vol. 21, no. 1, pp. 95–96, January 1975.